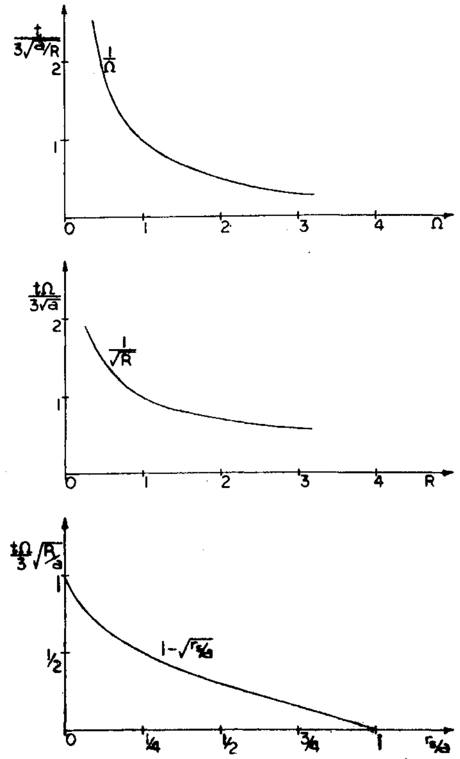

Fig. 3 Time of migration of bubble.

moving with the velocity U through a nonviscous liquid is given by potential theory as

$$v = \tfrac{3}{2}U \sin\theta \approx \tfrac{3}{2}U\theta \tag{7}$$

With this, the speed of migration of the bubble under the action of centrifugal force and under the lack of gravity is obtained by comparison of Eqs. (5) and (7) to be ($\delta = \frac{3}{2}$)

$$U = \tfrac{2}{3}\Omega(r_sR)^{1/2} \tag{8}$$

It may be seen from this that the speed of migration of a large bubble is proportional to the speed of rotation Ω and proportional to the square root of the distance of the stagnation point of the bubble from the axis of rotation. We conclude furthermore that it is proportional to the square root of the radius of curvature of the bubble, indicating that larger bubbles migrate faster (Fig. 2). For a small distance of the bubble from the axis of rotation its speed of migration is slow.

To determine the time of migration involved in the motion of a bubble, the following equation has to be integrated:

$$dr_s/dt = -\tfrac{2}{3}\Omega(Rr_s)^{1/2} \tag{9}$$

Assuming that the rotational speed Ω is kept constant and that the radius of curvature remains constant throughout the motion of migration, Eq. (9) yields

$$r_s = a - \tfrac{2}{3}\Omega(Ra)^{1/2}\cdot t + (\Omega^2/9)Rt^2 \tag{10}$$

where the distance of the stagnation point of the bubble from the rotational axis at the time $t = 0$ is considered to be $r_s(0) = a$. The time of migration from a to a location of the stagnation point of the bubble r_s is then

$$t = [3/\Omega(R)^{1/2}][(a)^{1/2} - (r_s)^{1/2}] \tag{11}$$

It may be seen that the time elapsing for a bubble moving from $r_s = a$ to the axis of rotation $r_s = 0$ is given by

$$t = 3(a)^{1/2}/\Omega(R)^{1/2} \tag{12}$$

which expresses (Fig. 3) that it is indirectly proportional to the rotational speed, proportional to the square root of the distance of the stagnation point of the bubble from the axis of rotation and indirectly proportional to the square root of the radius of curvature of the bubble. The larger the rotational speed, the earlier the bubble will reach the axis of rotation. A bubble of large radius of curvature shall reach the axis of rotation earlier than a bubble of small radius of curvature.

Electron Number Density at Shock Front due to Precursor Photoionization

S. S. R. Murty*
Indian Institute of Science, Bangalore-12, India

DOBBINS has presented the theory of shock precursors as applied to shock tube experiments in Ref. 1. He assumed black-body emission in the primary continuum from equilibrium region behind the shock which is likely to be violated as the initial pressure is lowered. We worked out this case in Ref. 2 and present here the main developments.

A review of the literature on shock precursor ionization is given by Pirri and Clarke.[3] Weymann,[4] Holmes and Weymann[5] presented experimental evidence for electron diffusion and photoionization as causing the observed precursors in shock tubes. They found that in any case photoionization dominates the near precursor.

The profile of electron number density ahead of the shock due to photoionization of atoms in ground state is described by

$$d(n_eu)/d\xi = -n_aQ_{13} \tag{1}$$

with the rate coefficient Q_{13} given by

$$Q_{13} = 4\pi \int_{\nu_1}^{\infty} \psi_{13}J_\nu d\nu \tag{2}$$

The notation is the same as in Ref. 6. The bound-free absorption coefficient a_ν decreases with frequency and can be represented by

$$a_\nu = P/\mu^n, \qquad \mu = \nu/\nu_1, \qquad a_\nu = \psi_{13}h\nu \tag{3}$$

$h\nu_1$ is the ionization potential. In Eq. (3), P and n are constants which depend on the particular atomic gas considered. We show later that the electron number density at the shock front due to photoionization is independent of both P and n. J_ν is the average spectral intensity given by

$$J_\nu = \left(\frac{1}{4\pi}\right)\int I_\nu d\omega \tag{4}$$

The intensity at any point A on the axis (Fig. 1) is

$$I_\nu(\xi,\theta) = B_\nu[1 - \exp(-K_\nu^{(2)}L \sec\theta)] \times \exp(-K_\nu^{(1)}\xi \sec\theta) \tag{5}$$

where B_ν is the Planck's function at the downstream equilibrium T_2. We have assumed LTE in the shock-heated gas and

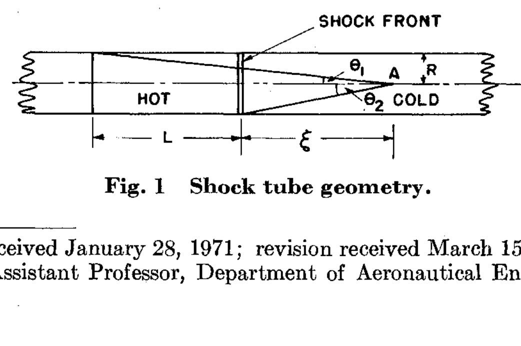

Fig. 1 Shock tube geometry.

Received January 28, 1971; revision received March 15, 1971.

* Assistant Professor, Department of Aeronautical Engineering.

included the ionizational relaxation region in the length L of the hot gas. For low Mach numbers, the relaxation region can be very large[7] and Eq. (5) for emergent intensity can be in error and must be used with caution. Superscripts (1) and (2) on the absorption coefficients $K_\nu = n_a a_\nu$ indicate that K_ν is evaluated at upstream and downstream conditions respectively. For high densities behind the shock, $K_\nu^{(2)}$ is large and one can approximate the shock-front emission in the primary continuum as that of a black body but use of Eq. (5) gives deviations from black-body when the density is not large enough. This formulation is based on LTE assumption which will not be true for very low densities. Within these limitations we can proceed further and obtain for the average intensity from Eqs. (4) and (5)

$$J_\nu = \tfrac{1}{2}B_\nu F(\tau_\nu) \tag{6}$$

where

$$F(\tau_\nu) = E_2(\tau_\nu) - E_2(\tau_\nu^{(L)} + \tau_\nu) - \frac{1}{Z_2}E_2(\tau_\nu Z_2) + \frac{1}{Z_1}E_2[(\tau_\nu^{(L)} + \tau_\nu)Z_1] + \int_{z_1}^{z_2}\frac{dZ}{Z^2}\exp\left[-\frac{\tau_\nu^{(R)}Z}{(Z^2-1)^{1/2}} + N\tau_\nu Z\right] \tag{7}$$

with

$$\tau_\nu = K_\nu^{(1)}\xi,\quad N = n_a^{(2)}/n_a^{(1)} - 1,\quad Z = \sec\theta,$$
$$\tau_\nu^{(L)} = K_\nu^{(2)}L,\qquad \tau_\nu^{(R)} = K_\nu^{(2)}R$$

It can be seen that $F(\tau_\nu)$ reduces to $E_2(\tau_\nu)$ for a plane shock wave of infinite extent by letting $\tau_\nu^{(L)}$, $\tau_\nu^{(R)}$ and $Z_2 \to \infty$.

Using Eq. (6), Q_{13} can be written as

$$Q_{13} = \frac{4\pi P\nu_1^3}{c^2}\int_1^\infty \mu^{2-n}F(\tau_\nu)\exp(-S\mu)d\mu \tag{8}$$

with $S = h\nu_1/KT_2$. Now we use Eq. (8) to substitute for Q_{13} in Eq. (1) and get the electron concentration as

$$n_e = \frac{4\pi\nu_1^3}{\mu c^2}\int_\eta^\infty d\eta\int_1^\infty \mu^{2-n}F\left(\frac{\eta}{\mu^n}\right)\exp(-S\mu)d\mu \tag{9}$$

where $\eta = n_a^{(1)}P\xi$. We treated $n_a^{(1)}$ and μ as constants in writing Eq. (9) which is justifiable.[8] Interchanging the order of integration in Eq. (9), we get

$$n_e = \frac{4\pi\nu_1^3}{uc^2}\int_1^\infty \mu^2\exp(-S\mu)G\left(\frac{\eta}{\mu^n}\right)d\mu \tag{10}$$

where

$$G\left(\frac{\eta}{\mu^n}\right) = E_3\left(\frac{\eta}{\mu^n}\right) - E_3\left[\left(\eta_2^{(L)} + \frac{\eta}{\mu^n}\right)\right] + E_3\left[(\eta_2^{(L)} + \eta)\frac{Z_1}{\mu^n}\right] - E_3\left[\left(\eta^2 + \frac{\eta_1^{(R)2}}{\mu^n}\right)^{1/2}\right] - \left(\frac{1}{N}\right)\int_{z_1}^{z_2}\frac{dZ}{Z^3}\exp\left[-\eta_2^{(R)}\frac{Z}{\mu^n}(Z^2-1)^{1/2} + \frac{NR\eta}{\mu^n}\right] + \left(\frac{1}{N}\zeta_2^2\right)E_3\left(\frac{\eta_1^{(R)}\zeta_2}{\mu^n}\right) \tag{11}$$

In Eq. (11), $\zeta_2 = \operatorname{cosec}\theta_2$, $\eta_2^{(L)} = n_a^{(2)}PL$, $\eta_2^{(R)} = n_a^{(2)}PR$ and $\eta_1^{(R)} = n_a^{(1)}PR$. The derivation of Eq. (11) is given in Ref. 2.

We will now try to check the order of magnitudes of η's appearing in Eq. (11). For argon at room temperature, we find $n_a^{(1)} = 3.2 \times 10^{16}p^{(1)}/\text{cm}^3$ where $p^{(1)}$ is mm Hg. Experimental results give $P = 34 \times 10^{-18}$ cm^2 for argon. The ratio of the number densities atoms before and after the shock is $n_a^{(2)}/n_a^{(1)} = (1-\alpha)\rho^{(2)}/\rho^{(1)}$. For purpose of estimation, we assume $n_a^{(2)} = 5n_a^{(1)}$ and obtain $n_a^{(2)}P = 5.45p^{(1)}$. For $L = 10$ cm, and $R = 2$ cm, we get $\eta_2^{(L)} = 54.5p^{(1)}$ and $\eta_2^{(R)} = 10.9p^{(1)}$. From these values, it is clearly seen that for initial pressures of $p^{(1)} \geq 1$ Torr, we can drop out terms containing $\eta_2^{(L)}$ and $\eta_2^{(R)}$ because of the exponential decay of the exponential integral function E_3. For $p^{(1)} = 0.1$ mm Hg, we find $\eta_2^{(L)} = 5.45$ and $\eta_2^{(R)} = 1.09$ and this is the pressure range for retaining $\eta_2^{(R)}$. For $p^{(1)} = 0.01$ mm Hg, corresponding to a pressure of the order of 10^{-5} atmosphere, both the terms $\eta_2^{(L)}$ and $\eta_2^{(R)}$ have to be retained.

For present day experiments with $p^{(1)} > 1$ mm Hg, one can approximate Eq. (11) as

$$G(\eta/\mu^n) \simeq E_3(\eta/\mu^n) - E_3[(\eta^2 + \eta_1^{(R)2})^{1/2}/\mu^n] + (1/N\zeta_2^2)E_3(\eta_1^{(R)}\zeta_2/\mu^n) \tag{12}$$

The magnitude of $\eta_1^{(R)}$ is now estimated. $\eta_1^{(R)} = n_a^{(1)}PR = 1.09p^{(1)}R$ for argon. Thus if $p^{(1)}R$ is greater than 5 Torr-cm, one can drop out terms containing $\eta_1^{(R)}$ in Eq. (12) since the present theory of ground state photoionization is valid only close to the shock front or more precisely for optical thickness $n_a^{(1)}P\xi$ less than about 5. For $p^{(1)}R > 5$ Torr-cm for argon, $G(\eta/\mu^n)$ tends to $E_3(\eta/\mu^n)$ indicating that the shock behaves like an infinite one even in shock tube as far as its behaviour in primary continuum is concerned. The same conclusions can be expected to be valid for resonance radiation also. However the subordinate continuum is usually optically thin and the shock front does not behave as an infinite one in this frequency range. For helium, $P \simeq 7 \times 10^{-18}$ cm^2 and at room temperature $n_a^{(1)} \simeq 3.2 \times 10^{17}p^{(1)}$ giving $\eta_1^{(R)} \simeq 2.25\,p^{(1)}R$. So it is enough if $p^{(1)}R > 2$ for the shock to behave as an infinite one in helium in the primary continuum.

For values of $p^{(1)}R$ lower than those indicated, one must use Eq. (12) for $G(\eta/\mu^n)$ in Eq. (10). Then we find that integrals of the form

$$\int_1^\infty \mu^2\exp(-S\mu)E_3\left(\frac{\beta}{\mu^n}\right)d\mu \tag{13}$$

have to be handled with β denoting a function of η independent of μ. It may be noted that as μ increases, β/μ^n decreases and we need an accurate representation of $E_3(t)$ in the range 0–β where $t = \beta/\mu^n$. The usual practice is to approximate it by an exponential function and then use the method of steepest descent. However, a simpler thing to do in view of the form of the integrand is to express $E_3(\beta/\mu^n)$ in power series accurate enough over the range 0–β. We expect β to be less than 5 in the range of validity of this theory. Thus we express

$$E_3(t) = \sum_{j=0}^{m} a_j t^j \tag{14}$$

where the m constants a_j can be found to the desired accuracy by curve fitting. Using Eq. (14), we get from Eq. (10) and Eq. (12)

$$n_e = \frac{4\pi\nu_1^3}{uc^2}\left\{\frac{a_0H}{N\zeta_2^2} + \sum_{j=1}^{m}a_jE_{nj-2}(S)\times\left[\eta - (\eta^2 + \eta_1^{(R)2})^{j/2} + \left(\frac{1}{N}\zeta_2^2\right)(\eta_1^{(R)}\zeta_2)^j\right]\right\} \tag{15}$$

Here $H = (1/S)(1 + 2/S + 2/S^2)\exp(-S)$ and we assumed that n is an integer and $nj \geqslant 2$. If n is not integral, it is not always possible to write a closed form expression. Eq. (15) describes the decay of electron number density in the precursor region.

For a plane infinite shock wave, one has only the first term on the right side of Eq. (12) and we obtain

$$n_e = \frac{4\pi\nu_1^3}{uc^2}\left[a_0H + \sum_{j=1}^{m}a_j\eta^j E_{nj-2}(S)\right] \tag{16}$$

The number density at the shock front itself denoted by n_{e0}

can be obtained exactly from Eqs. (10) and (12) by setting $\eta = 0$ or from Eq. (16) with $a_0 = \frac{1}{2}$ since $E_3(0) = \frac{1}{2}$. The result is

$$n_{e0} = (2\pi\nu_1^3/uc^2)(1/S)(1 + 2/S + 2/S^2)\exp(-S) \quad (17)$$

n_{e0} is seen to be independent of the values of atomic constants P and n and depends only on the frequency ν_1 at the edge of the primary continuum. This result is physically obvious for the steady, infinite shock case since all of the photons for $\nu > \nu_1$ are absorbed, independent of the magnitude or form of the spectral absorption coefficient. The exact values of P and n are required only for the subsequent decay of the electron number density. This prediction that the electron number density at shock front due to photoionization being dependent only on ν_1 can be checked if measurements are made on different atomic gases. We attempted to compare the theoretical results with Holmes and Weymann's measurements in Ref. 2 but the comparisons are of doubtful value in view of several uncertainties.[7]

References

1 Dobbins, R. A., "Precursor Photoexcitation and Photoionization of Argon in Shock Tubes," *AIAA Journal*, Vol. 8, No. 3, March 1970, pp. 407–413.

2 Murty, S. S. R., "Electron Number Density at Shock Front Due to Photoionization," Rept. AE 275, June 1970, Department of Aeronautical Engineering, Indian Institute of Science, Bangalore-12, India.

3 Pirri, A. N. and Clarke, J. H., "Radiative Ionization Patterns in Cold Precursor of Axisymmetric Detached Shock," *AIAA Journal*, Vol. 8, No. 9, Sept. 1970, pp. 1574–1581.

4 Weymann, H. D., "Precursors Ahead of Shock Waves: I. Electron Diffusion," *The Physics of Fluids*, Vol. 12, No. 6, June 1969, pp. 1193–1199.

5 Holmes, L. B. and Weymann, H. D., "Precursors Ahead of Shock Waves: II. Photoionization," *The Physics of Fluids*, Vol. 12, No. 6, June 1969, pp. 1200–1210.

6 Murty, S. S. R., "Effect of Line Radiation on Precursor Ionization," *Journal of Quantitative Spectroscopy and Radiative Transfer*, Vol. 8, No. 1, Jan. 1968, pp. 531–554.

7 Dobbins, R. A., private communication, July 1970, Brown University, Providence, R. I.

Base Pressure Correlation in Supersonic Flow

M. W. Su* and J. M. Wu†

The University of Tennessee Space Institute
Tullahoma, Tenn.

Base drag can be a significant fraction of the total drag of a body flying at supersonic speeds. The estimation of the base pressure has received a great deal of attention. However, because of the complicated and coupled nature of the near wake, no satisfactory correlation parameter for accurately predicting the base pressure for flow with transition in the wake has yet been found. In this note, a correlation parameter is identified and proposed, which is derived on the basis of the reduced Reynolds number in the mixing region.

Received January 25, 1971; revision received March 12, 1971 Work supported under U.S. Air Force Contracts AF33615-67-1758 and 33615-70-C-1645.

* Graduate Research Assistant; now Senior Engineer, Boeing Company, Space Division, Huntsville, Ala. Member AIAA.

† Associate Professor of Aerospace Engineering, Member AIAA.

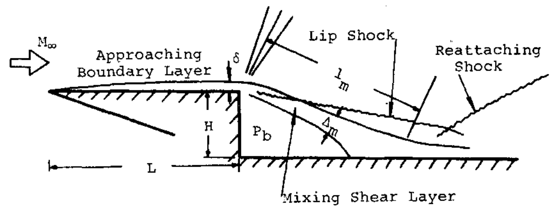

Fig. 1 Sketch of base flow field.

In a locally separated region, the usually defined Reynolds number based on the characteristic length of a body is rather ambiguous and does not yield a proper physical meaning. To a base flow (see Fig. 1), one may easily sense that the characteristic length for such type of flow is the total mixing shear length l_m and the mixing width Δ_m at near the recompression region. An attempt was made to correlate the base pressure to these two lengths. A very encouraging base pressure correlation was obtained. The only difficulty is that the l_m and the Δ_m lengths are not known a priori. Therefore, one must find a way to relate these two lengths to the known body lengths; namely, the model length upstream of a two-dimensional rearward facing step L and the step height H. Physically, the length L is related to the boundary-layer thickness δ prior to separation which will influence the mixing width Δ_m and the step height H which is related to the mixing shear length l_m.

The ratio of inertia to viscous forces in the mixing shear layer, or the physically correct reduced Reynolds number Re_c in this region, may be expressed as,

$$Re_c = \rho_\infty U_\infty(U_\infty/l_m)/\mu_\infty(U_\infty/\Delta_m^2) = (\rho_\infty U_\infty l_m/\mu_\infty)(\Delta_m/l_m)^2 \quad (1)$$

where l_m and Δ_m are taken as the characteristic dimensions of the mixing region as discussed. The estimation of l_m and Δ_m is often difficult. If one assumes that

$$l_m \sim H \quad (2)$$

$$\frac{\Delta_m}{\delta} \sim \left(\frac{l_m}{\delta}\right)^n \sim \left(\frac{H}{\delta}\right)^{n(Re_{\infty,L},M_\infty)} \quad (2a)$$

where the exponent n is a function of freestream Reynolds number based on L and the freestream Mach number M_∞. The exponent n may depend strongly on whether the mixing shear layer is laminar, transitional or turbulent. Based on (2) and (2a), the reduced Reynolds number Re_c of Eq. (1)

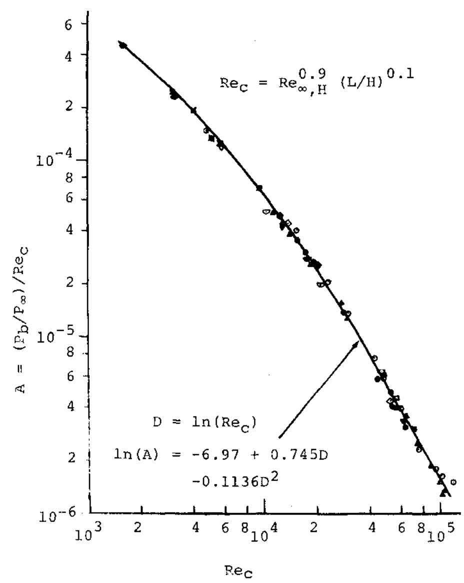

Fig. 2 Base pressure correlation for rearward facing step.